Available online at www.sciencedirect.com
ScienceDirect
Nuclear Physics A 00 (2015) 1–4
Nuclear Physics A
www.elsevier.com/locate/procedia

arXiv:1512.07631v1 [nucl-th] 23 Dec 2015

Observable consequences of event-by-event fluctuations of HBT radii

Christopher Plumberg and Ulrich Heinz

Physics Department, The Ohio State University, 191 W. Woodruff Ave, Columbus, OH 43210

Abstract

We explore the effects of event-by-event fluctuations of Hanbury Brown–Twiss (HBT) radii and show how they can be observed experimentally. The relation of measured HBT radii extracted from ensemble-averaged correlation functions to the mean of their event-by-event probability distribution is clarified. We propose a method to experimentally determine the mean and variance of this distribution and test it on an ensemble of fluctuating events generated with the viscous hydrodynamic code VISH2+1. Using the same code, the sensitivity of the mean and variance of the HBT radii to the specific QGP shear viscosity η/s is studied. We report sensitivity of the mean pion HBT radii and their variances to the temperature dependence of η/s near the quark-hadron transition at a level similar (10-20%) to that which was previously observed for elliptic and quadrangular flow of charged hadrons [1].

Keywords:

1. Introduction

For the past several years, event-by-event fluctuations in the initial conditions of heavy-ion collisions have played a critical role in our understanding of how these collisions evolve. Their manifestations have been studied extensively by means of a wide variety of momentum-space observables, such as the mean transverse momenta $\langle p_T \rangle$ and the anisotropic flow coefficients v_n, which all fluctuate from event to event. The fluctuations of these observables are characterized by probability distributions over a set of collision events with tightly constrained collision geometries; different moments of these distributions are accessible with different observables.

We here extend the study of these fluctuations by exploring their effect on HBT interferometry. In contrast to flow measurements, which reflect the momentum-space structure of the final state of a heavy-ion collision, measurements of HBT radii provide insight into its space-time structure. By finding a way to characterize the event-by-event distribution of fluctuating HBT

radius parameters with a set of measurements that determine a few of its moments, we hope to obtain insights into the fluctuations of the size and shape of the collision fireballs at freeze-out. Theoretical modeling of these HBT fluctuations can establish to what extent measuring their moments can provide additional information about the properties of the medium whose evolution connects the observed final state with the fluctuating initial state – information that, being based on a spatio-temporal measurement of the final state, may be complementary to that extracted from flow measurements.

2. Formalism

For an ensemble of events, the normalized and ensemble-averaged two-particle correlation function, for a pair of momenta $\vec{p}_1$ and $\vec{p}_2$, is defined experimentally by

$$C_{\rm avg}(\vec{p}_1,\vec{p}_2) \equiv \frac{\left\langle E_{p_1}E_{p_2}\frac{d^6N}{d^3p_1 d^3p_2}\right\rangle_{\rm ev}}{\left\langle E_{p_1}\frac{d^3N}{d^3p_1}\right\rangle_{\rm ev}\left\langle E_{p_2}\frac{d^3N}{d^3p_2}\right\rangle_{\rm ev}}. \tag{1}$$

Using the Gaussian source approximation to write the HBT radii in terms of space-time variances of the source [2–4], the radii associated with the correlation function (1) can be shown [5] to be an event-multiplicity-weighted average of the HBT radii of the individual events in the ensemble:

$$R^2_{\langle ij\rangle}(\vec{K}) \equiv \left\langle wR^2_{ij}\right\rangle_{N_{\rm ev}} \equiv \frac{\sum_{k=1}^{N_{\rm ev}} N_k^2(\vec{K})\left(R^2_{ij}(\vec{K})\right)_k}{\sum_{k=1}^{N_{\rm ev}} N_k^2(\vec{K})}, \quad \text{where} \quad N_k(\vec{K}) \equiv \left(E_K\frac{d^3N}{d^3K}\right)_k. \tag{2}$$

$N_k(\vec{K})$ is the multiplicity of particles with momentum $\vec{K}$ in the kth event, and the weights in the average represent the number of pairs with pair momentum $\vec{K}$ contributed by each event to the ensemble-averaged correlation function. We refer to these ensemble-averaged radii as their *physical ensemble average* (PEA); this PEA is measured in the experiments. The PEA differs in general from the simple arithmetic average of the radius parameters in the measured ensemble,

$$\left\langle R^2_{ij}(\vec{K})\right\rangle_{N_{\rm ev}} \equiv \frac{1}{N_{\rm ev}}\sum_{k=1}^{N_{\rm ev}}\left(R^2_{ij}(\vec{K})\right)_k, \quad \text{where} \quad \langle O\rangle_{N_{\rm ev}} \equiv \frac{1}{N_{\rm ev}}\sum_{k=1}^{N_{\rm ev}} O_k\,. \tag{3}$$

We refer to Eq. (3) as the *direct ensemble average* (DEA). Denoting the distribution of event-by-event radii for an ensemble of events formally by $\mathcal{P}_{N_{\rm ev}}(R^2_{ij})$, the DEA radii represent its *true* mean whereas the PEA radii represent a weighted mean. No technique exists currently to correct the measured PEA radii to obtain a good estimate for the DEA radii.

To further characterize $\mathcal{P}_{N_{\rm ev}}(R^2_{ij})$ (which cannot be measured directly because limited pair multiplicities make a full HBT analysis of individual events impossible), we can try to determine also a few of its higher statistical moments, e.g., its variance $\sigma^2_{ij,N_{\rm ev}} \equiv {\rm Var}\left[\mathcal{P}_{N_{\rm ev}}(R^2_{ij})\right]$. In [5] we have proposed the following set of techniques for experimentally constructing estimates for both the DEA mean $\left\langle R^2_{ij}\right\rangle_{N_{\rm ev}}$ and the variance $\sigma^2_{ij,N_{\rm ev}}$ of the ensemble distribution of radii $\mathcal{P}_{N_{\rm ev}}(R^2_{ij})$:

1. To estimate the DEA radii for an ensemble containing $N_{\rm ev}$ events, we sort the events by increasing multiplicity $N(\vec{K})$, split them into $\tilde{n}_b$ bins of $\tilde{n} \equiv N_{ev}/\tilde{n}_b$ events each, and compute the PEA radii $\langle wO\rangle^{(\ell)}_{\tilde{n}}$ for the sub-ensembles corresponding to each bin $\ell = 1,\ldots,\tilde{n}_b$. If n_b is sufficiently large (but still $n_b \ll N_{\rm ev}$), the weights may be treated as approximately

constant within each bin, implying that $w_k^{(\tilde{n})} \approx \frac{\tilde{n}_b}{N_{ev}}$. With this approximation one shows that [5]

$$\langle O \rangle_{N_{ev},\mathrm{est}} \equiv \frac{1}{\tilde{n}_b} \sum_{\ell=1}^{\tilde{n}_b} \langle wO \rangle_n^{(\ell)} \approx \langle O \rangle_{N_{\mathrm{ev}}} \,. \tag{4}$$

2. To estimate the variance, we begin again with an ensemble containing N_{ev} events, and we consider an iterative procedure consisting of the following two steps. For the kth iteration, we first split the N_{ev} events into n_b equally-sized sub-ensembles, and estimate the DEA radii $\left\langle R_{ij}^2 \right\rangle_{k,\ell}$ for each of these sub-ensembles ($\ell = 1, \ldots, n_b$). We then compute the variance of these n_b estimates for the DEA radii, which in turn yields an estimate for the variance of the distribution of DEA radii of sub-ensembles of size $n \equiv N_{\mathrm{ev}}/n_b$. Iterating these steps M times thus generates M variance estimates which we then average and rescale by a factor determined by the central limit theorem, finally obtaining the following estimate for $\sigma^2_{ij,N_{\mathrm{ev}}}$:

$$\sigma^2_{ij,N_{\mathrm{ev}},\mathrm{est}} \equiv \frac{N_{\mathrm{ev}}/n_b}{M(n_b-1)} \sum_{k=1}^{M} \sum_{\ell=1}^{n_b} \left(\left\langle R_{ij}^2 \right\rangle_{k,\ell}^2 - \left\langle R_{ij}^2 \right\rangle_{N_{\mathrm{ev}}}^2 \right). \tag{5}$$

3. Results

We now use these techniques to estimate the relative widths $\sigma_{ij}/\langle R_{ij}^2 \rangle_{N_{\mathrm{ev}}}$ of an ensemble of $N_{\mathrm{ev}} = 5000$ 200A GeV Au+Au events at 0-10% centrality. Further details of our analysis are provided in [5, 6]. Fixing $n_b = 2$ in Eq. (5), we obtain the estimates for the relative widths shown in the top left part of Fig. 1. We see that increasing $\tilde{n}_b$ decreases the bias of our estimator, while increasing M decreases the variability and improves the statistical precision.

To illustrate possible useful applications of our proposed techniques we demonstrate the sensitivity of the relative widths of $R_o^2 \left(\sigma_o / \langle R_o^2 \rangle_{N_{\mathrm{ev}}} \right)$ to the value of the specific shear viscosity η/s in the quark-gluon plasma (QGP) phase of heavy-ion collision evolution. These results are shown in the lower lefthand panel of Fig. 1. The observed increase of $\sigma_o/\langle R_o^2 \rangle_{N_{\mathrm{ev}}}$ at large K_T can be shown [6] to result primarily from event-by-event fluctuations of the emission duration, not the emission geometry, while the decrease with increasing η/s can be understood as a suppression of event-by-event fluctuations due to the increased dissipation in the hydrodynamic evolution.

This intuition is confirmed in the right part of Fig. 1 where we show, for three values of the pair momentum $\vec{K}$ and three different choices of the specific shear viscosity η/s in the hydrodynamic evolution, the regions of greatest emissivity along the freeze-out surface for a typical fluctuating event in our ensemble. Red regions represent strongest particle emission, and blue regions the weakest. For small K_T (top row), the effective emission regions are clearly centered at small radii and late times, while for larger K_T values (middle and bottom rows) the effective emission regions shift toward larger radii and earlier times. As the freeze-out surface fluctuates from event to event, due to the generic shape of the freeze-out surface the emission regions at large K_T are constrained to fluctuate primarily in the temporal (vertical) direction and not much in the radial (transverse) direction. This implies that, at large K_T, fluctuation signatures will tend to be dominated by emission duration over emission geometry, as stated above. Moreover, a comparison of the ideal results in the lefthand column ($\eta/s = 0$) with the viscous results in the middle and righthand columns ($\eta/s = 0.08$ and 0.2) reveals a clear suppression of the bumpiness of the freeze-out surface as η/s is increased, leading to the reduced variance of the HBT radii

seen in the lower left panel of Fig. 1. We conclude that the new observables proposed here can indeed yield valuable additional insights into heavy-ion collisions and their evolution.

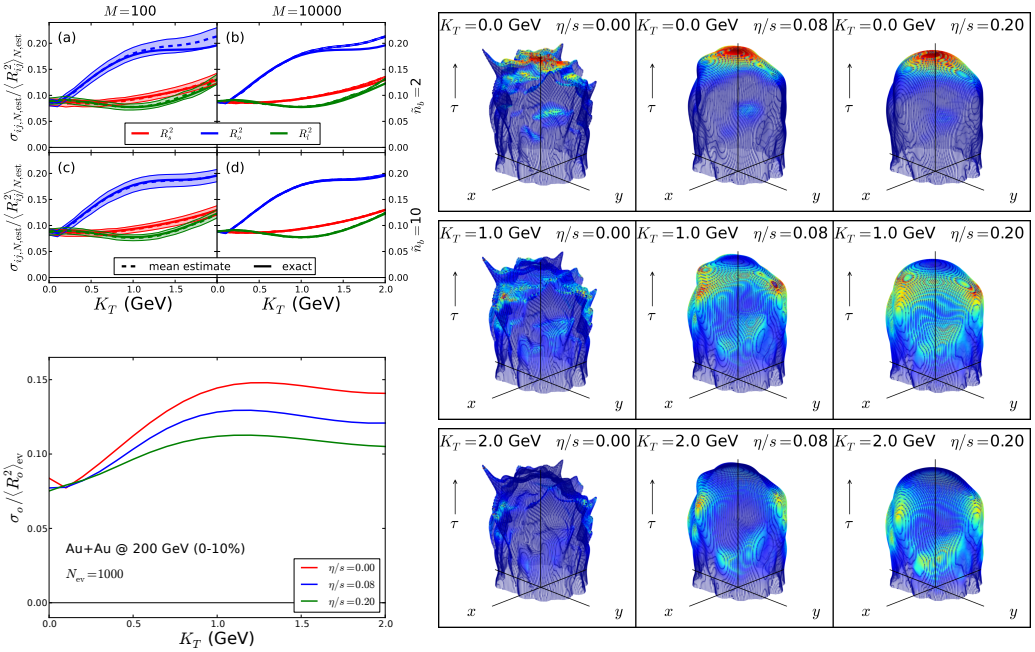

Fig. 1. **Top left:** Comparison of estimated relative widths $\sigma_{ij,N_{\rm ev}}/\langle R_{ij}^2\rangle_{N_{\rm ev}}$ with their exact values as functions of K_T, for 5000 0-10% Au+Au events at 200A GeV, for $M = 100$, 10000 (left vs. right) and $\bar{n}_b = 2$, 10 (top vs. bottom), using $n_b = 2$. **Bottom left:** Exact relative widths $\sigma_{o,N_{\rm ev}}/\langle R_o^2\rangle_{N_{\rm ev}}$ as function of K_T for 1000 0-10% Au+Au events at 200A GeV, using $(\eta/s)_{QGP} = 0.00$, 0.08, and 0.20 as indicated. **Right:** Effective emission regions on the fluctuating freeze-out surface for a single event with fixed bumpy initial conditions, for different values of the pair momentum K_T (rows) and for hydrodynamic evolution with different $(\eta/s)_{QGP}$ values (columns).

Acknowledgements: We thank Jai Salzwedel and Michael Lisa for valuable discussions. This work was supported by the Department of Energy, Office of Science, Office of Nuclear Physics under Awards No. DE-SC0004286 and (within the framework of the JET Collaboration) DE-SC0004104. Computing resources provided by the Ohio Supercomputer Center [7] are gratefully acknowledged.

References

[1] E. Molnar, H. Holopainen, P. Huovinen, H. Niemi, Phys. Rev. C90 (2014) 044904.
[2] U. Heinz. arXiv:hep-ph/0407360.
[3] U. Heinz, B. V. Jacak, Ann. Rev. Nucl. Part. Sci. 49 (1999) 529–579.
[4] U. A. Wiedemann, U. Heinz, Phys. Rept. 319 (1999) 145–230.
[5] C. Plumberg, U. Heinz, Phys. Rev. C92 (2015) 044906.
[6] C. Plumberg, U. Heinz, Phys. Rev. C91 (2015) 054905.
[7] Ohio Supercomputer Center, `http://osc.edu/ark:/19495/f5s1ph73` (1987).